

Adaptive hp-Polynomial Based Sparse Grid Collocation Algorithms for Piecewise Smooth Functions with Kinks

Hendrik Wilka and Jens Lang

Technical University Darmstadt, Department of Mathematics

Dolivostraße 15, 64293 Darmstadt, Germany

wilka@mathematik.tu-darmstadt.de, lang@mathematik.tu-darmstadt.de

May 26, 2025

Abstract

High-dimensional interpolation problems appear in various applications of uncertainty quantification, stochastic optimization and machine learning. Such problems are computationally expensive and request the use of adaptive grid generation strategies like anisotropic sparse grids to mitigate the curse of dimensionality. However, it is well known that the standard dimension-adaptive sparse grid method converges very slowly or even fails in the case of non-smooth functions. For piecewise smooth functions with kinks, we construct two novel *hp*-adaptive sparse grid collocation algorithms that combine low-order basis functions with local support in parts of the domain with less regularity and variable-order basis functions elsewhere. Spatial refinement is realized by means of a hierarchical multivariate knot tree which allows the construction of localised hierarchical basis functions with varying order. Hierarchical surplus is used as an error indicator to automatically detect the non-smooth region and adaptively refine the collocation points there. The local polynomial degrees are optionally selected by a greedy approach or a kink detection procedure. Four numerical benchmark examples with different dimensions are discussed and comparison with locally linear, quadratic and highest degree basis functions are given to show the efficiency and accuracy of the proposed methods.

Key words. adaptive sparse grid collocation, multi-dimensional interpolation, discontinuities, hp-adaptivity, greedy algorithm, kink detection, hierarchical multi-scale method

1 Introduction

The efficient approximation of high-dimensional functions has become a fundamental component in almost all scientific fields. Prominent areas are uncertainty quantification,

stochastic optimization and machine learning. For example, the quantitative characterization of uncertainties in certain outcomes, if some input parameters are stochastically modelled, typically leads to high-dimensional problem spaces in which interpolation operations need to be performed. The use of full tensor grids is often not feasible since the number of grid points increases exponentially, i.e., $O(M^N)$ for M grid points in each of the N dimensions – the well-known curse of dimensionality. Sparse grids have emerged as an extremely useful tool box offering the possibility to only select grid points that contribute most to the multi-dimensional approximation of the solution [7, 16, 18]. The complexity of the sparse grid method reduces to $O(M \log(M)^{N-1})$ [4]. By taking advantage of higher smoothness and dimension-dependent adaptivity, which was originally proposed in [8] as anisotropic grids and further developed in [11, 13], even faster rates of convergence can be achieved. Given appropriate error estimators, this generalized sparse grid method automatically concentrates grid points in important dimensions.

However, when the function to be approximated exhibits a non-smooth dependence on the uncertain input parameters, sparse grid methods that use a global polynomial basis can not efficiently resolve local kinks or discontinuities in the random space. In such cases, spatial refinement has to be added to boost the efficiency of sparse grid approximations. Locally adaptive sparse grids were first investigated in [9] for the numerical solution of PDEs. So-called h -adaptive generalized sparse grid methods have been used in [12] with multi-linear hierarchical basis functions of local support and in [10] with a higher, but fixed maximum polynomial degree. The magnitude of the hierarchical surplus, i.e. the difference between the function and its approximation at a newly selected grid point not yet part of the current point set, guides the spatial refinement. More recently, a generalized spatially adaptive sparse grid combination technique with dimension-wise refinement was proposed in [14]. Simplex stochastic collocation for piecewise smooth functions with kinks was analysed in [5]. Although, all these methods achieve a fast rate of convergence in smooth regions and acceptable accuracies around discontinuities or kinks, a combination of local h - and p -adaptivity in the spirit of the hp -version of the finite element method which often shows exponential convergence has not been utilised so far.

Thus, we exploit the localised polynomial basis proposed in [3] to construct an hp -adaptive generalized sparse grid method. Local polynomial basis functions of different degree can be constructed by means of so-called ancestor knots. With the help of the hierarchical surplus, we adopt the local polynomial degree to the local regularity of the function. We have developed two approaches: (1) The greedy approach derives an individual score for all possible polynomial degrees and chooses the one with the minimal interpolation error calculated at newly selected collocation points. (2) The kink detection approach based on a polynomial annihilation technique [1, 2] is applied to identify regions with discontinuous first derivatives. Then, piecewise linear basis functions are used there. New collocation points are investigated locally around an active set of already chosen points and added to that set until a given threshold for the hierarchical surplus is reached.

The paper is organised as follows. In Section 2, we introduce the fundamentals of adaptive hierarchical sparse grids based on localised hierarchical basis functions with varying

order. Our novel *hp*-generalised sparse grid algorithm is described in Section 3. Numerical results for four benchmark functions and comparison to other approaches are presented in Section 4. We summarize our results in Section 5.

2 Adaptive hierarchical sparse grids

We are interested in interpolating non-smooth functions $f : \Omega \rightarrow \mathbb{R}$ defined on an N -dimensional bounded domain Ω . Without loss of generality, we choose $\Omega = [-1, 1]^N$ and require that f can be evaluated at arbitrary points in Ω . Our main focus will be on piecewise smooth functions that have kinks along certain manifolds.

2.1 From univariate interpolation to hierarchical sparse grids

Let us start with univariate interpolation on the interval $I = [-1, 1]$. For a given index $l \in \mathbb{N}_0$, we consider m_l knots $-1 \leq y_1^{(l)} < \dots < y_{m_l}^{(l)} \leq 1$ with the corresponding set of knots

$$Y_l := \left\{ y_1^{(l)}, \dots, y_{m_l}^{(l)} \right\}, \quad l \in \mathbb{N}_0.$$

We assume $m_{l+1} \geq m_l$ for different levels of interpolation. A knot-based interpolation operator $\mathcal{U}^{(l)}$ is now given by

$$\mathcal{U}^{(l)}(f)(x) = \sum_{j=1}^{m_l} f(y_j^{(l)}) \phi_j^{(l)}(x), \quad x \in I,$$

where $\phi_j^{(l)}$, $j = 1, \dots, m_l$, are basis functions which satisfy $\phi_j^{(l)}(y_k^{(l)}) = \delta_{jk}$. Hence, $\mathcal{U}^{(l)}(f)$ is exact on the given interpolation knots.

Defining the multiindex $\mathbf{l} = (l_1, \dots, l_N)$ and $Y_{\mathbf{l}} = Y_{l_1} \times \dots \times Y_{l_N}$ with knot sets Y_{l_1}, \dots, Y_{l_N} for each dimension, we get the multivariate interpolation operator

$$\begin{aligned} \mathcal{U}^{(\mathbf{l})}(f)(\mathbf{x}) &= \left(\mathcal{U}^{(l_1)} \times \dots \times \mathcal{U}^{(l_N)} \right) (f)(\mathbf{x}) \\ &= \sum_{j_1=1}^{m_{l_1}} \dots \sum_{j_N=1}^{m_{l_N}} f(y_{j_1}^{(l_1)}, \dots, y_{j_N}^{(l_N)}) \left(\phi_{j_1}^{(l_1)} \cdot \dots \cdot \phi_{j_N}^{(l_N)} \right) (\mathbf{x}), \quad \mathbf{x} \in \Omega. \end{aligned} \quad (1)$$

Again, this construction satisfies the interpolation property $\mathcal{U}^{(\mathbf{l})}(f)(y_{\mathbf{j}}^{(\mathbf{l})}) = f(y_{\mathbf{j}}^{(\mathbf{l})})$ for all $y_{\mathbf{j}}^{(\mathbf{l})} = (y_{j_1}^{(l_1)}, \dots, y_{j_N}^{(l_N)}) \in Y_{\mathbf{l}}$. Since the number of interpolation knots in the full-tensor product (1) grows very quickly, we apply a sparse grid interpolation based on the Smolyak algorithm [16]. Assuming nested point sets $Y_l \subset Y_{l+1}$ for $l \in \mathbb{N}_0$, we introduce new point sets

$$X_0 := Y_0, \quad X_l := Y_l \setminus Y_{l-1}, \quad l \geq 1.$$

With $X_l = \{x_1^{(l)}, \dots, x_{|X_l|}^{(l)}\}$, we have $x_j^{(l)} = y_{j'}^{(l)}$ for some j' . On the other hand, for every $y_j^{(l)}$ there exist a unique pair (l', j') such that $y_j^{(l)} = x_{j'}^{(l')}$, since $Y_l = \cup_{k=1, \dots, l} X_k$. Further, the corresponding incremental interpolation operators

$$\Delta^{(l)} = \mathcal{U}^{(l)} - \mathcal{U}^{(l-1)}, \quad l \in \mathbb{N}_0,$$

with the convention $\mathcal{U}^{(-1)} \equiv 0$ has the property

$$\Delta^{(l)}(f)(x_j^{(l)}) = \mathcal{U}^{(l)}(f)(x_j^{(l)}) - \mathcal{U}^{(l-1)}(f)(x_j^{(l)}) = f(x_j^{(l)}) - \mathcal{U}^{(l-1)}(f)(x_j^{(l)})$$

and therefore $\Delta^{(l)}(f)(x_j^{(l')}) = 0$ for $l' < l$. Following [12, Sec. 3.3], we get the well-known relation

$$\Delta^{(l)}(f) = \sum_{x_j^{(l)} \in X_l} \left(f(x_j^{(l)}) - \mathcal{U}^{(l-1)}(f)(x_j^{(l)}) \right) \varphi_j^{(l)} =: \sum_{x_j^{(l)} \in X_l} w_j^{(l)} \varphi_j^{(l)}. \quad (2)$$

Here, $w_j^{(l)}$ is the one-dimensional hierarchical surplus representing the difference between the function values at the current and the previous interpolation levels. The set of functions $\varphi_j^{(l)}$ are now defined as the hierarchical basis functions.

Using the identity $\sum_{k=0, \dots, l} \Delta^{(k)} = \mathcal{U}^{(l)}$, the full-tensor approximation (1) can be decomposed into

$$\begin{aligned} \mathcal{U}^{(l)} &= \mathcal{U}^{(l_1)} \times \dots \times \mathcal{U}^{(l_N)} = \left(\sum_{l_1=0}^w \Delta^{(l_1)} \right) \times \dots \times \left(\sum_{l_N=0}^w \Delta^{(l_N)} \right) \\ &= \sum_{l_1=0}^w \dots \sum_{l_N=0}^w \Delta^{(l_1)} \times \dots \times \Delta^{(l_N)} =: \sum_{l: \|l\|_\infty \leq w} \Delta^{(l)} \end{aligned} \quad (3)$$

for any $w \in \mathbb{N}_0$. Defining $L := |l| = \sum_{d=1, \dots, N} l_d$, the classical sparse grid interpolation operator originally introduced in [16] is given by

$$\mathcal{A}_q(f) = \sum_{l: L \leq q} \Delta^{(l_1)}(f) \times \dots \times \Delta^{(l_N)}(f)$$

for some maximum order $q \geq N$. Equivalently, we can use Smolyak's formula [7, 16]

$$\mathcal{A}_q(f) = \sum_{l: q-N+1 \leq L \leq q} (-1)^{q-L} \binom{N-1}{q-L} \left(\mathcal{U}^{(l_1)}(f) \times \dots \times \mathcal{U}^{(l_N)}(f) \right) \quad (4)$$

to get a representation without incremental operators. For M knots per dimension, we have M^N function evaluations in the full-tensor approximation (1), which grows exponentially with the dimension N and hence suffers from the curse of dimensionality. Sparse

grids reduce the number of points to $\mathcal{O}(M \log(M)^{N-1})$ while keeping a comparable approximation quality for smooth functions [4]. Obviously, the curse of dimensionality is significantly delayed, but not broken. Further improvements can be made by adaptive strategies, i.e., only adding knots that reduce the interpolation error efficiently [8, 13]. However, problems with non-smooth functions f require spatial refinement and the use of low order basis functions in parts of the domain with less regularity. A generalized sparse grid approach which allows such an improvements will be described next.

2.2 Hierarchical basis functions with local support

In order to identify and resolve local non-smooth variations of the function f , detection algorithm and spatial refinement can be performed on the level of a single hierarchical basis function $\varphi_j^{(l)}$ from (2). We consider one-dimensional equidistant points of the sparse grid which can be considered as a tree-like data structure [3, 4]. Let an equidistant knot set Y_l on $[-1, 1]$ given by

$$\begin{aligned} x_1^{(0)} &= 0, \\ x_j^{(1)} &= 2j - 3, \quad j = 1, 2 =: |X_1| \\ x_j^{(l)} &= (2j - 1)2^{1-l} - 1, \quad j = 1, \dots, 2^{l-1} =: |X_l|, \quad l \geq 2. \end{aligned} \quad (5)$$

For these knots, we can define a hierarchical structure: We start with a central knot, $x_1^{(0)} = 0$. This knot has the two child knots $x_1^{(1)} = -1$ and $x_2^{(1)} = 1$ located at the boundary of the interval. These knots have the child knots $x_1^{(2)} = -\frac{1}{2}$ and $x_2^{(2)} = \frac{1}{2}$, respectively. From now on, the child knots can be defined recursively. Every knot $x_j^{(l)}$ with $l \geq 2$ has two child knots with the positions $x_j^{(l)} \pm 2^{-l}$. In the following, $S_C(x_j^{(l)})$ denotes the children set of a knot $x_j^{(l)}$. Further, let $S_P(x_j^{(l)})$ be the parent of a knot, which always exists for $l \geq 1$. We have

$$x_{j'}^{(l-1)} = S_P(x_j^{(l)}) \Leftrightarrow x_j^{(l)} \in S_C(x_{j'}^{(l-1)}).$$

With that, we can also define the set of unique ancestors $S_A(x_j^{(l)}) := \{x_{j_{l-1}}^{(l-1)}, x_{j_{l-2}}^{(l-2)}, \dots, x_1^{(0)}\}$ that satisfy

$$S_P(x_j^{(l)}) = x_{j_{l-1}}^{(l-1)}, S_P(x_{j_{l-1}}^{(l-1)}) = x_{j_{l-2}}^{(l-2)}, \dots, S_P(x_{j_1}^{(1)}) = x_1^{(0)}.$$

The resulting structure forms a knot tree, see Fig. 1 for an illustration with $l = 4$.

We will now define designated supports for local hierarchical basis functions. Let $s_j^{(l)} := \text{supp } \varphi_j^{(l)}$ and set

$$\begin{aligned} s_1^{(0)} &= [-1, 1], \quad s_1^{(1)} = [-1, 0], \quad s_2^{(1)} = [0, 1], \\ s_j^{(l)} &= \left[x_j^{(l)} - 2^{1-l}, x_j^{(l)} + 2^{1-l} \right], \quad l \geq 2. \end{aligned} \quad (6)$$

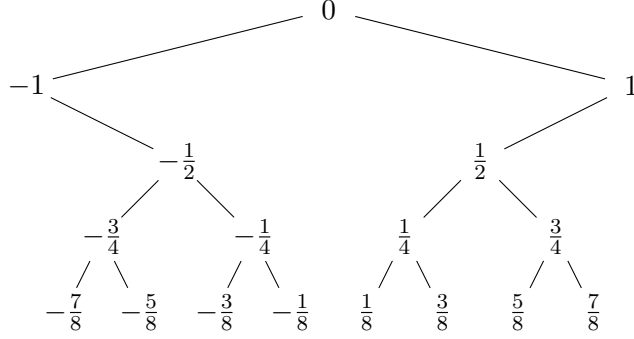


Figure 1: The first 5 levels of the equidistant knot tree on $[-1, 1]$. For example, the ancestors of knot $x = -\frac{5}{8}$ are $S_A(-\frac{5}{8}) = \{-\frac{3}{4}, -\frac{1}{2}, -1, 0\}$.

This yields

$$s_{j_1}^{(l)} \cap s_{j_2}^{(l)} = \begin{cases} \{x_{j'}^{(l')}\} & \text{with } l' < l, \quad \text{if } |j_1 - j_2| = 1 \\ \emptyset, & \text{if } |j_1 - j_2| > 1 \end{cases}.$$

Thus, supports of knots in the same level intersect at most in one point. Additionally, the supports are nested and respect the hierarchical structure of the knots, i.e.,

$$x_j^{(l)} \in S_C(x_{j'}^{(l-1)}) \Rightarrow s_j^{(l)} \subset s_{j'}^{(l-1)}.$$

A new basis function $\varphi_j^{(l)}$ modifies an existing interpolation only in the support of its parent and $\varphi_j^{(l)}, \varphi_{j'}^{(l)}$ with $j \neq j'$ do not influence each other.

The parent-child relation for knots can be extended to the multivariate case by defining the sets of children

$$S_C(x_{\mathbf{j}}^{(l)}) := \left\{ \left(x_{j_1}^{(l_1)}, \dots, x_{j_{d-1}}^{(l_{d-1})}, x, x_{j_{d+1}}^{(l_{d+1})}, \dots, x_{j_N}^{(l_N)} \right) : x \in S_C(x_{j_d}^{(l_d)}) \text{ for } d = 1, \dots, N \right\}$$

for $\mathbf{l} = (l_1, \dots, l_N)$ and $\mathbf{j} = (j_1, \dots, j_N)$. Observe that each multivariate knot can have at most $2N$ children and multiple parents along different axes.

Local polynomial basis functions of high degree can be constructed by means of ancestor knots as originally studied in [3]. Let $N=1$ and $l > 2$. Then, we use knots from $S_A(x_j^{(l)})$ to define a higher-order basis function $\varphi_j^{(l)}$ of the difference operator $\Delta^{(l)}$ associated to the knot $x_j^{(l)}$ and satisfying

$$\varphi_j^{(l)}(x_j^{(l)}) = 1, \quad \varphi_j^{(l)}(x_{j'}^{(l')}) = 0 \text{ for all } x_{j'}^{(l')} \in S_A(x_j^{(l)}).$$

We note that the boundary points of the support $s_j^{(l)}$ of $\varphi_j^{(l)}$ are also included in $S_A(x_j^{(l)})$. Further ancestors lie outside of $s_j^{(l)}$. The definition of the local higher-order basis functions is consistent in the sense that a global interpolant built up with them fulfills all requirements of a hierarchical Lagrangian interpolation. The new weight is given by $w_j^{(l)} = f(x_j^{(l)}) - \mathcal{I}^{(l-1)}(x_j^{(l)})$, where $\mathcal{I}^{(l-1)}$ denotes the interpolation operator that uses knots up to level $l-1$. The number of ancestors knots used defines the degree of $\varphi_j^{(l)}$. To reach order p , we take the knot $x_j^{(l)}$, its two ancestors a_1, a_2 at the boundary of $s_j^{(l)}$, and additionally its nearest $p-2$ ancestors a_3, \dots, a_p ordered by their distance to $x_j^{(l)}$. The new basis function is then defined by

$$\varphi_j^{(l)}(x) := \varphi_{j,p}^{(l)}(x) = \begin{cases} \prod_{k=1}^p \frac{x - a_k}{x_j^{(l)} - a_k} & , x \in s_j^{(l)}, \\ 0 & , x \notin s_j^{(l)}. \end{cases} \quad (7)$$

With a predefined maximum degree p_{\max} , we will consider the set of basis functions

$$\Phi_j^{(l)} := \left\{ \varphi_{j,p}^{(l)}, p = 2, \dots, \min\{p_{\max}, l\} \right\}. \quad (8)$$

It remains to choose basis functions for $l \leq 2$. For the root knot $x_1^{(0)}$, we take the constant function $\varphi_{1,0}^{(0)} \equiv 1$. In the case $l=1$, linear basis functions $\varphi_{1,1}^{(1)}(x)$, $\varphi_{2,1}^{(1)}(x)$ on $s_1^{(1)}$, $s_2^{(1)}$ defined in (6) are chosen, respectively. Eventually, the quadratic polynomial $\varphi_{j,2}^{(2)}(x)$ vanishing at the boundary of the support is taken for $l=2$. But, we will also use the piecewise linear basis function $\varphi_{j,1}^{(2)}(x)$ as defined for $l=1$.

Generalized multivariate basis functions of degree $\mathbf{p} = (p_1, \dots, p_N) \in \mathbb{N}^N$ are now defined as products

$$\varphi_{\mathbf{j},\mathbf{p}}^{(l)}(\mathbf{x}) := \varphi_{j_1,p_1}^{(l_1)}(x_1) \cdot \dots \cdot \varphi_{j_N,p_N}^{(l_N)}(x_N) \quad (9)$$

of one-dimensional basis functions, where \mathbf{p} satisfies $p_i \leq \min\{p_{\max}, l_i\}, i = 1, \dots, N$, and $|\mathbf{l}| \leq q \in \mathbb{N}$. We note that resulting global interpolants are continuous functions on Ω .

Remark 2.1 In [3], the use of one $p := p_{\max}$ for all directions is called the p -regular scenario. For functions f having bounded mixed derivatives up to order $p+1$ in the L^q -norm, $q \in \{2, \infty\}$, and vanishing on the boundary of $\bar{\Omega} := [0, 1]^N$, the L^∞ - and L^2 -error of the p -regular sparse grid approximation is of order $\mathcal{O}(h_n^{p+1} |\log_2 h_n|^{N-1})$, $h_n = 2^{-n}$, if $n \geq p$ [4, Theorem 4.8]. This shows a higher-order approximation.

Multi-linear hierarchical basis functions, i.e. $p = 1$ in all directions, of local support have been successfully applied in [12]. Especially for discontinuous functions, this approach leads to a significant reduction in the number of collocation points required to

achieve comparable accuracy as classical, possibly dimension-adaptive sparse grid collocation methods. Linear adaptive methods, however, put often an unnecessarily large number of points in region where the solution is smooth. An h -adaptive generalised sparse grid method (h -GSG) with fixed maximum degree p_{\max} , which is based on the above localised polynomial basis and the magnitude of the hierarchical surplus, has been proposed in [10]. It achieves a fast rate of convergence in smooth regions and accuracies around discontinuities or kinks that are comparable to those of linear methods.

Remark 2.2 *An error analysis in [10] reveals that if $\|f - \mathcal{U}_{\text{opt}}(f)\| \leq \varepsilon$ with the least number of function evaluations to construct the (optimal) interpolant $\mathcal{U}_{\text{opt}}(f)$, then the h -adaptive GSG approximation $\mathcal{U}_N(f)$ satisfies $\|f - \mathcal{U}_N(f)\| \leq \varepsilon(1 + C(\varepsilon))$, where $C(\varepsilon)$ is the number of points that are used in $\mathcal{U}_{\text{opt}}(f)$, but not in $\mathcal{U}_N(f)$. $C(\varepsilon)$ depends on the smoothness of f : the smoother f the smaller $C(\varepsilon)$ will be.*

2.3 Localised hierarchical basis functions with varying order

Although the support $s_j^{(l)}$ of the one-dimensional basis function $\varphi_{j,p}^{(l)}$ gets smaller for larger l due to its definition in (6), ancestors of $x_j^{(l)}$ also lie outside for $p > 2$. This bears difficulties in the approximation quality when higher-order Lagrangian interpolation is applied across regions of less regularity as discontinuities or kinks of the function to be approximated.

For an illustration, let us consider the function

$$f(x) = \begin{cases} 0 & , x \leq r \\ \sin\left(\frac{x-r}{1-r}\pi\right) & , x > r \end{cases} \quad (10)$$

with a kink at $r = -0.45$. From Fig. 2 it becomes clear that the basis function for the knot $x_1^{(3)} = -0.75$ at level $l = 3$ uses function values from ancestor knots lying on both sides of the kink, which yields an unsatisfactory approximation in its support $[-1, -0.5]$. Adding further points near the kink will only slowly reduce the interpolation error. Detecting the kink at an early stage by e.g. a greedy approach explained in Section 3.1 overcomes this undesired behaviour. Here, basis functions with support away from the kink are constructed using knots on one side of the kink only.

3 The hp -generalised sparse grid algorithm

Here, we will departure from previous work in the literature and use localised hierarchical basis functions with varying order. It is our goal to combine the strengths of both local h - and p -adaptivity in a generalised sparse grid method shortly denoted by hp -GSG.

Let A denote the active set of adaptively chosen knots $x_{j'}^{(l')}$ used at level q , $q \geq |l'|$ for all l' selected, to construct the interpolant $\mathcal{U}_A^{(q)}(f)$. Then the weight at each child knot

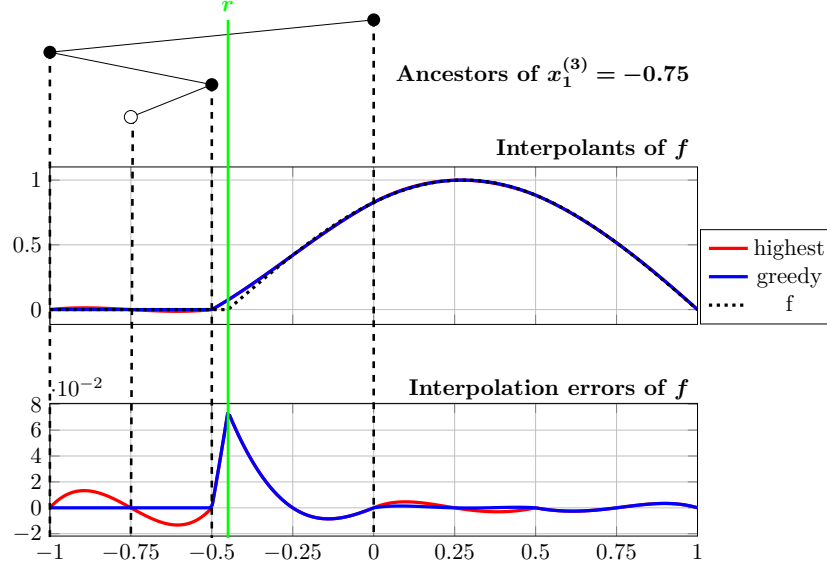


Figure 2: Interpolation across a kink for f defined in (10). The basis function $\varphi_{1,3}^{(3)}$ at knot $x_1^{(3)} = -0.75$ with *highest* possible polynomial degree $p = 3$ uses a function value at $x = 0$, which leads to a relatively bad approximation of $f(x) \equiv 0$ in its support $[-1, -0.5]$ away from the kink at $x = -0.45$. The *greedy* approach described in Section 3.1 restricts the used ancestors and yields a zero error there.

$x_j^{(l)} \in S_C(x_{j'}^{(l')})$ with $|\mathbf{l}'| = q$ can be computed by

$$w_j^{(l)} = f(x_j^{(l)}) - \mathcal{U}_A^{(q)}(f)(x_j^{(l)}).$$

The new function values $f(x_j^{(l)})$ can be used to adopt the current polynomial degree of the previously defined basis functions $\varphi_{j'}^{(l')}$, $|\mathbf{l}'| = q$. This is done in the subroutine *Modification*. If a child knot is added to the active set A , i.e., we find $|w_j^{(l)}| \geq w_{\max}$ with a certain threshold w_{\max} , a new basis function $\varphi_j^{(l)}$ with an appropriate polynomial degree is defined in the subroutine *Selection*. Both routines will be explained in the next subsections. The whole structure of the novel *hp*-GSG algorithm is outlined in Algorithm 1. For a better readability, we use „evaluate“ for a function evaluation at a certain knot.

3.1 Greedy approach

For a knot $x_j^{(l)} = (x_{j_1}^{(l_1)}, \dots, x_{j_N}^{(l_N)}) \in A$, the one-dimensional basis function $\varphi_{j_d, p_d}^{(l_d)}(x_d)$ used in (9) has to be chosen from the set $\Phi_{j_d}^{(l_d)} \cup \{\varphi_{j_d, 1}^{(l_d)}\}$ defined in (8) and thereafter. We want to optimize all previously chosen p_d in such a way that the interpolation error at some test knots is as small as possible. Whenever new child knots are considered in the *hp*-GSG

Algorithm 1: *hp-generalised sparse grid approximation*

Input: Function $f(x)$, minimum level q_{\min} , maximum level q_{\max} , threshold w_{\max} , maximum polynomial degree p_{\max}

Result: Grid \mathcal{G} with knots $x_j^{(l)}$, weights $w_j^{(l)}$, basis functions $\varphi_j^{(l)}$

begin

Set $x_1^{(0)} := \mathbf{0}$ and evaluate it.

Set $A_0 := \{x_1^{(0)}\}$, $\mathcal{G} = A_0$, $q := 1$.

while $q \leq q_{\max}$ **do**

Set the child set $C = \emptyset$.

for Every knot $x_{j'}^{(l')} \in A_{q-1}$ **do**

Add every child knot in $S_C(x_{j'}^{(l')})$ to C and evaluate them.

Define $\varphi_{j'}^{(l')} := \text{MODIFICATION}(\mathbf{l}', j')$.

end

for Every child $x_j^{(l)} \in C$ **do**

Calculate the weight $w_j^{(l)}$ for $x_j^{(l)}$.

if $q \leq q_{\min}$ or $|w_j^{(l)}| \geq w_{\max}$ **then**

Add $x_j^{(l)}$ to A_q .

Define $\varphi_j^{(l)} := \text{SELECTION}(\mathbf{l}, j)$.

end

end

Set $\mathcal{G} := \mathcal{G} \cup A_q$

end

end

method, the two new function values for varying $x_{j_d}^{(l_d)}$, which have to be calculated in any case, can be used to derive a score for all possible polynomial degrees. Remembering $\varphi_{j_i, p_i}^{(l_i)}(x_{j_i}^{(l_i)}) = 1$, $1 \leq i \leq N$, we set

$$S_p := \max_{x \in S_C(x_{j_d}^{(l_d)})} \left| \mathcal{W}^{(l_d-1)}(x) + w_{j_d}^{(l_d)} \varphi_{j_d, p}^{(l_d)}(x) - f(x) \right|, \quad p = 1, \dots, \max\{p_{\max}, l_d\},$$

and choose a new $p_d := \arg \min_p S_p$. Note that $\mathcal{W}^{(l_d-1)} + w_{j_d}^{(l_d)} \varphi_{j_d, p_d}^{(l_d)}$ is the local interpolation in level l_d if one would choose p_d as polynomial degree. Finally, N individual optimization steps are performed to find $\mathbf{p} = (p_1, \dots, p_N)$. This greedy-like strategy is implemented in *Modification* in Algorithm 1.

In the subroutine *Selection*, appropriate polynomial degrees have to be chosen for basis functions $\varphi_j^{(l)}$ defined for a selected child knot $x_j^{(l)} \in A_q$ on the highest level $q = |\mathbf{l}|$. Suppose

$x_j^{(l)}$ was added by changing $x_{j_d}^{(l'_d)}$ in its parent knot $x_{j'}^{(l')}$ along the d -axis. Then we set $p_d := \min\{p'_d + 1, p_{\max}\}$ and replace $\varphi_{j'_d, p'_d}^{(l'_d)}(x_d)$ by $\varphi_{j_d, p_d}^{(l_d)}(x_d)$ in $\varphi_{j'}^{(l')}$ to define the new basis function for the child knot.

With these definitions of the subroutines, the hp -GSG is uniquely determined. For later use, we call it hp -GSG-g, where „g“ stands for **g**reedy.

3.2 Kink detection approach

Here, we would like to combine our hp -GSG method with a kink detection procedure as described in [1, 2]. Although the greedy approach is in principle able to detect any unsmoothness of the function f , a kink detection might be preferable if it is a priori known that f exhibits kinks, i.e., discontinuities in its first derivatives.

We will first recapitulate the main points of the derivative discontinuity detection method [1] and then describe its incorporation into our sparse grid algorithm. It is sufficient to consider the one-dimensional case and apply the procedure on each axis separately.

Let f be a continuous function with well defined left and right side limits. Assume that $f \in C^1(I \setminus \Theta)$ with $I := [-1, 1]$ and Θ being the discrete set of jump discontinuities in the first derivative. For each $x \in I$, we define the usual jump function

$$[f'](x) := \lim_{x_+ \searrow x} f'(x_+) - \lim_{x_- \nearrow x} f'(x_-).$$

We have $[f'](\xi) \neq 0$ for $\xi \in \Theta$ and $[f'](x) = 0$ otherwise. It is the goal to construct an approximation of $[f'](x)$ that rapidly converges to zero away from $\xi \in \Theta$. Consider a point $x \in I$ and a stencil $\mathcal{S}_x = \{x_0, \dots, x_{m+2}\}$ of its nearest $m + 3$ grid points with $x_0 < \dots < x_{m+2}$, $m > 1$, and known values $f(x_i)$. We define

$$\mathcal{S}_x^+ := \{x_i : x_i \geq x\} \quad \text{and} \quad \mathcal{S}_x^- := \mathcal{S}_x \setminus \mathcal{S}_x^+.$$

and assume $|\mathcal{S}_x^+|, |\mathcal{S}_x^-| > 1$ to have sufficient information left and right of $x \in I$. Let k with $1 \leq k < m + 1$ such that $x_j \in \mathcal{S}_x^-$ for $j \leq k$ and $x_j \in \mathcal{S}_x^+$ for $j > k$. Further, define the maximum separation length $h_x := \max\{|x_i - x_{i-1}| : x_i, x_{i-1} \in \mathcal{S}_x\}$. An approximation of $[f'](x)$ is now defined by

$$L_{m, \mathcal{S}_x} f(x) = h_x^{m-1} \sum_{i=0}^{m+2} c_i f(x_i),$$

where the coefficients c_i are uniquely determined through the system of linear equations, see [2, Theorem 2.1],

$$\begin{aligned} c_0 p_l(x_0) + \dots + c_{m+2} p_l(x_{m+2}) &= p_l^{(m)}(x), \quad l = 0, \dots, m, \\ c_{k+1} p_l(x_{k+1}) + \dots + c_{m+2} p_l(x_{m+2}) &= h_x^{1-m} p_l^{(1)}(x), \quad l = 0, 1. \end{aligned}$$

Here, p_0, \dots, p_m is a basis of the space of all polynomials up to degree m and $p_l^{(k)}$ denotes the k -th derivative of p_l . We choose $p_l(x) = x^l \in \Pi_m$ as basis and apply the algorithm from [2, Appendix A] to calculate the coefficients c_i , $i = 0, \dots, m+2$. Note that $c_i = \mathcal{O}(h_x^{-m})$.

In [2, Corollary 2.5], it was shown that for the special case when $x_i \leq x, \xi \leq x_{i+1}$ for some $x_i \in \mathcal{S}_x$, i.e., the discontinuity point ξ and the reconstruction point x lie within the same cell, and ξ being the only jump discontinuity in the smallest closed interval I_x that contains \mathcal{S}_x , then it holds

$$L_{m, \mathcal{S}_x} f(x) = [f'](\xi) + \mathcal{O}(h_x^{\min(\kappa, m)})$$

for piecewise smooth $f \in C^\kappa(I_x \setminus \{\xi\})$, $\kappa > 1$. Hence, the approximation $L_{m, \mathcal{S}_x} f(x)$ converges to $[f'](\xi)$ with a rate depending on m and the local smoothness of f .

Remark 3.1 *As explained in [2] in a heuristic manner, the derivative discontinuity detection method is based on a polynomial annihilation technique. If the function f is smooth in I_x , then $L_{m, \mathcal{S}_x} f(x)$ will annihilate all terms in the Taylor expansion of f up to degree $\kappa - 1$ by construction of the c_i . Since the residual of the Taylor expansion is bounded, multiplication with the scaling factor h_x^{m-1} produces an error which is proportional to the density of the sampled points. Hence, there is a high order of convergence in smooth regions, whereas function values on both sides of x , i.e., in \mathcal{S}_x^- and \mathcal{S}_x^+ , allow the approximation of the derivative discontinuity in the point x when f has a kink there.*

In the setting of knot trees, a slight modification is necessary at the boundary. Let $x_0 < x$ be the only point available in \mathcal{S}_x^- and p the interpolating polynomial in \mathcal{S}_x with $|\mathcal{S}_x| = 3$, i.e., two further knots right of x are available, then we define

$$L_{\mathcal{S}_x} f(x) := p'(x) - \frac{p(x) - f(x_0)}{x - x_0}$$

as approximation of $[f'](x)$. The analogous expression is used at the right boundary.

We will now explain the use of the kink detection in our hp -GSG method. It is important to identify a kink as fast as possible in order to select suitable basis functions. Hence, we apply the approach in the subroutine *Selection* of Algorithm 1. Suppose $x_j^{(l)}$ was added by changing $x_{j_d}^{(l_d)}$ in its parent knot $x_j^{(l')}$ along the d -axis. For levels $q \leq 2$, no kink detection is performed since there are only a few points available. If $q > 2$, we compute $\eta_d := |L_{m, \mathcal{S}_x} f(x_{j_d}^{(l_d)})|$ using the $m+2 := 4$ nearest knots to $x := x_{j_d}^{(l_d)}$ along the d -axis and the knot itself such that $x_0 < x_1 < x < x_3 < x_4$. If $\eta_d > w_{\text{kink}}$ with a certain threshold w_{kink} , we conclude that a kink is detected in the one-dimensional support $s_{j_d}^{(l_d)}$ and hence we choose the piecewise linear basis function $\varphi_{j_d, 1}^{(l_d)}$ there. Otherwise, we set $s_{j_d}^{(l_d)} = \varphi_{j_d, p_d}^{(l_d)}$ with $p_d := \min\{p_d' + 1, p_{\max}\}$, where p_d' is the degree of the basis function of the corresponding parent knot. It might happen in our adaptive algorithm that there are not enough points along a certain axis to perform a kink detection. However, in this case

we expect the interpolation error to be very small there and again choose the piecewise linear basis function.

Eventually, the subroutine *Modification* is skipped, i.e., no modification for parent knots takes place. For later use, we call this method *hp*-GSG-k, where „k“ stands for **k**ink detection.

4 Numerical examples

We will investigate the performance of the newly proposed *hp*-GSG methods compared to three already existing approaches: choosing always (i) locally linear basis functions as in [12], (ii) locally quadratic basis functions with anisotropic inspection of the sparse grid indices as favoured in [10] for non-smooth functions, and (iii) highest degree basis functions first proposed in [3], referred to as „linear“, „quadratic“ and „highest“. The strategies „linear“ and „highest“ are special cases of Algorithm 1, whereas programming „quadratic“ requires some adaptation. In the latter case, the threshold w_{max} refers to the ε that controls the error indicators in [10, Formula (8)]. The algorithms have been programmed using C++ and Matlab. We have used the Matlab-Version R2024a on an Intel Xeon Gold 6130 CPU. For time measurements, an average over three runs was taken.

The following functions which have been considered in previous work [10, 12, 17] are used:

$$f_0(x) = \frac{1}{|0.3 - x_1^2 - x_2^2| + 0.1}, \quad x \in [0, 1]^2,$$

$$f_1^N(x) = \exp\left(-\sum_{i=1}^N a_i |x_i - 0.51|\right), \quad x \in [0, 1]^N, \quad a_i = 2^{3-i}, i = 1, \dots, N,$$

$$f_2^N(x) = \prod_{i=1}^N \frac{4|x_i^2 - 0.66^2| + a_i}{a_i + 1}, \quad x \in [0, 1]^N, \quad a_1 = 0.5, \quad a_i = (i-1)^2, i = 2, \dots, N,$$

$$f_3^N(x) = \begin{cases} 0 & \text{if } \max\{x_1, x_2\} > 0.51 \\ \exp\left(\sum_{i=1}^N a_i x_i\right) & \text{else} \end{cases}, \quad x \in [0, 1]^N, \quad a_i = 2^{3-i}, i = 1, \dots, N.$$

The first problem is a well established benchmark problem with a one-dimensional kink that is not aligned with a certain coordinate axis. Clearly, the standard dimension-adaptive (anisotropic) sparse grid method fails in this case since it cannot resolve such non-smooth functions, see the discussion in [12, Chapter 4.1]. The function $f_1^N(x)$ is taken from the continuous family of the Genz library [6]. We set for the dimension $N = 2, 10, 50$. Eventually, we consider a modified g-function $f_2^N(x)$ of Sobol [15] with quadratic terms x_i^2 instead of linear ones and set $N = 2, 5$. As a robustness check, we also consider a discontinuous function $f_3^N(x)$ from the Genz library [6] for $N = 2, 5$. In all cases, we choose the parameters a_i in such a way to mimic a decreasing importance of the directions

x_i . Note that we use 0.51 in the definition of f_1^N and f_3^N for the characterization of the kinks and discontinuities, respectively, to avoid a direct alignment with the knots.

The error is measured in the following norms:

$$\epsilon_\infty := \max_{i=1,\dots,M} \left| f(x^{(i)}) - \mathcal{U}_A^{(q)}(f)(x^{(i)}) \right|,$$

$$\epsilon_2 := \left(\frac{1}{M} \sum_{i=1}^M \left| f(x^{(i)}) - \mathcal{U}_A^{(q)}(f)(x^{(i)}) \right|^2 \right)^{1/2},$$

with randomly chosen test points $x^{(i)} \in \Omega$, $i = 1, \dots, 10^5$, and additional 10^3 points $x^{(j)}$ along the kinks. Here, f and $\mathcal{U}_A^{(q)}(f)$ denote the true function and its interpolant, respectively.

We set $p_{\max} = 6$, $q_{\min} = 1$, and $q_{\max} = 25$ in Algorithm 1 for all numerical tests, except for f_0 , where we use $q_{\max} = 30$.

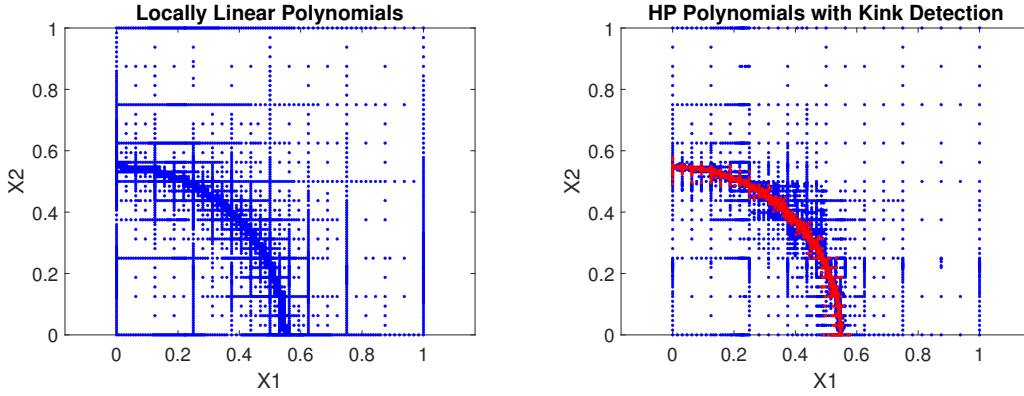


Figure 3: Test problem with f_0 . Knot placement for locally linear polynomials (left) and hp -GSG-k (right) with thresholds $w_{\max} = 10^{-3}$ and $w_{\text{kink}} = 5$. Knots of basis functions for which a kink was detected within an interval of size smaller than 2^{-6} are colored in red.

4.1 Approximation of f_0

The function f_0 exhibits a regularized line singularity along the circle around $(0,0)$ with radius $r = \sqrt{0.3}$. The gradients close to this line are quite large, which motivates a larger threshold $w_{\text{kink}} = 5$ for the kink detection. We use $w_{\max} = 10^{-2i+1}$, $i = 2, \dots, 6$, for „quadratic“ and $w_{\max} = 10^{-i}$, $i = 1, \dots, 4$, for all other methods. In Figure 3, the knot placement for locally linear polynomials (method „linear“) and hp -GSG-k with thresholds $w_{\max} = 10^{-3}$ is shown. The kink detection is able to identify the region of interest and places less grid points in smooth regions due to the higher-order polynomials used there.

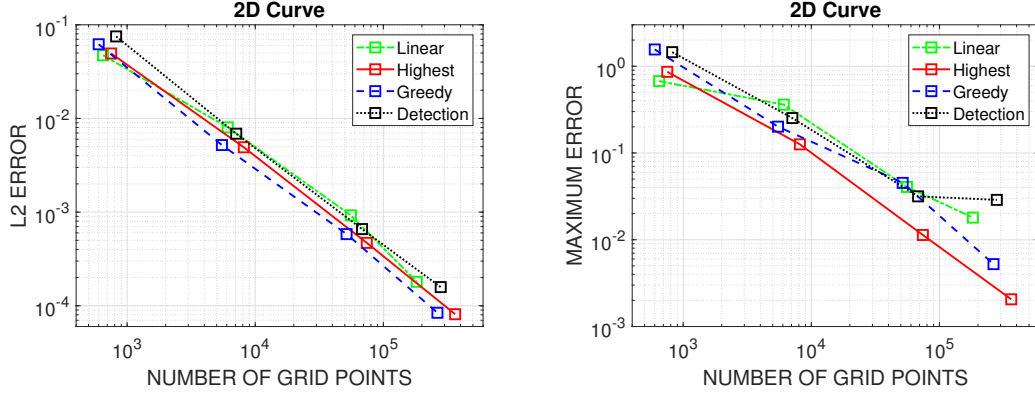


Figure 4: Test problem with f_0 . Comparison of the errors ϵ_2 (left) and ϵ_∞ (right).

However, the advantage of the *hp*-strategy in terms of accuracy is less pronounced as can be seen from the error plots in Figure 4. All methods perform quite similar for the 2-norm, whereas the simple strategy „highest“ and the more sophisticated „quadratic“ are best for the ∞ -norm closely followed by *hp*-GSG-g. This example verifies that methods with local refinement deliver comparably accurate results. A closer look at the computing time shows that all methods perform equally well with respect to achieved accuracy. Therefore, we omit the details.

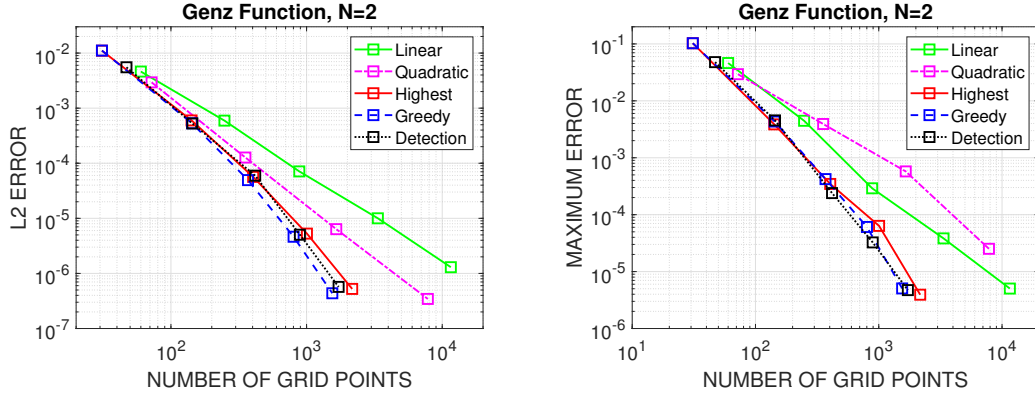


Figure 5: Test problem with f_1^2 . Comparison of the errors ϵ_2 (left) and ϵ_∞ (right).

4.2 Approximation of f_1^N in various dimensions

Now we consider the function f_1^N which has kinks of decreasing importance along the coordinate axis. For dimension $N = 2$, we use $w_{\max} = 10^{-4}, 6 \cdot 10^{-7}, 3 \cdot 10^{-9}, 10^{-11}$, for „quadratic“ and a sequence of 5 thresholds $w_{\max} = 10^{-i}, i = 2, \dots, 6$, for all other methods. For $N = 10, 50$, we choose $w_{\max} = 10^{-i}, i = 2, \dots, 5$, for „quadratic“ and

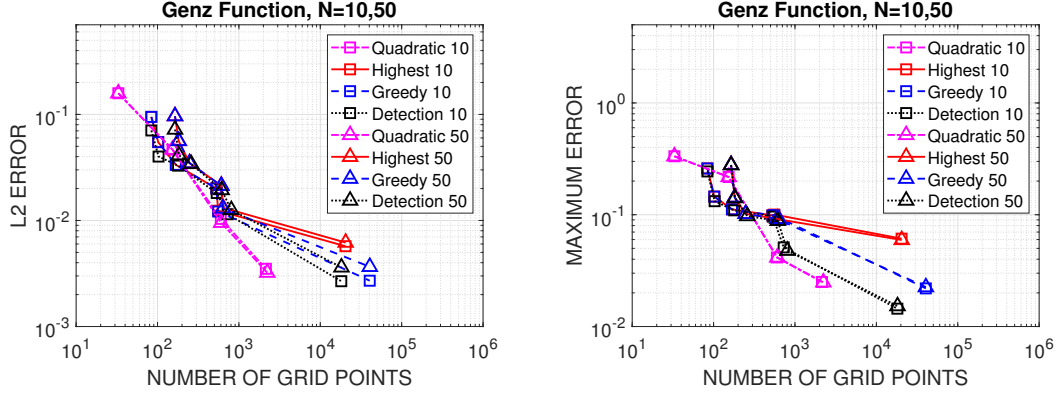


Figure 6: Test problem with $f_1^{10,50}$. Comparison of the errors ϵ_2 (left) and ϵ_∞ (right).

$w_{\max} \in [3 \cdot 10^{-3}, 10^{-1}]$ for 6 different runs else. The threshold for the kink detection is fixed with $w_{\text{kink}} = 1$. The corresponding convergence results are plotted in Figure 5 and Figure 6. For $N = 2$, both newly designed hp -GSG methods perform better than the other three for both error measures, ϵ_2 and ϵ_∞ . Further, the additional effort of „quadratic“ to detect anisotropic features does not pay off. The strategy „linear“ is no longer able to compete, which becomes even more evident for higher dimensions. We therefore omit its results for $N = 10, 50$. In these cases, the new methods outperform „highest“ for higher accuracies. For higher tolerances, „quadratic“ is the best method. However, in terms of computing time versus the accuracy achieved in the 2-norm, it is less efficient for $N = 2, 10$, as can be seen in Figure 7. The new approaches work equally well for $N = 2$. They still outperform „highest“ in higher dimensions, but they are less efficient for higher accuracies and $N = 50$ than „quadratic“. The ability to detect anisotropies is very useful here. Similar observations are made for the ∞ -norm.

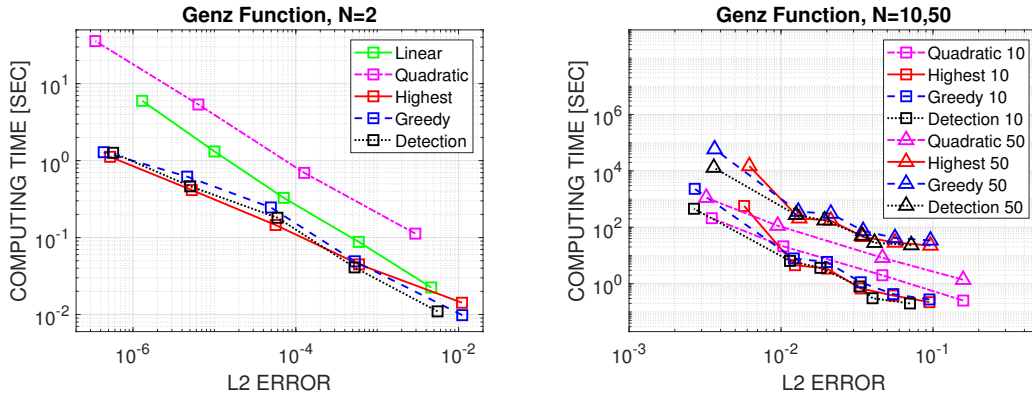


Figure 7: Test problem with f_1^N . Comparison of computing time in seconds versus accuracy in the 2-norm for $N = 2$ (left) and $N = 10, 50$ (right).

4.3 Approximation of f_2^N in various dimensions

Next we consider the function f_2^N for $N = 2, 5$. For each index i , a lower value of a_i indicates a higher importance of the variable x_i . The threshold w_{\max} for „quadratic“ varies in $[10^{-13}, 10^{-4}]$ for $N = 2$ and is set to 10^{-i} , $i = 3, \dots, 7$, for $N = 5$. For the other methods, we use $w_{\max} = 10^{-i}$, $i = 2, \dots, 6$, for $N = 2$ and five varying values in $[10^{-3}, 10^{-1}]$ for $N = 5$. The threshold for the kink detection is again fixed with $w_{\text{kink}} = 1$. In Figure 8 and Figure 9, the convergence results are shown for ϵ_2 and ϵ_∞ . For $N = 2$, the greedy approach hp -GSG-g and „quadratic“ perform best, whereas for $N = 5$, hp -GSG-k is equally good. The advantage of these methods compared to „linear“ and „highest“ is clearly visible and quite impressive for $N = 2$ and higher accuracies. Once again, the strategy „linear“ needs too much knots for $N = 5$. Therefore, the corresponding results are not shown in Figure 9. The superiority of the new methods for $N = 2$ is clearly reflected in the computing time shown in Figure 10 as function of the 2-error. For $N = 5$, all methods except „linear“ perform quite the same. The same holds true for the maximum error.

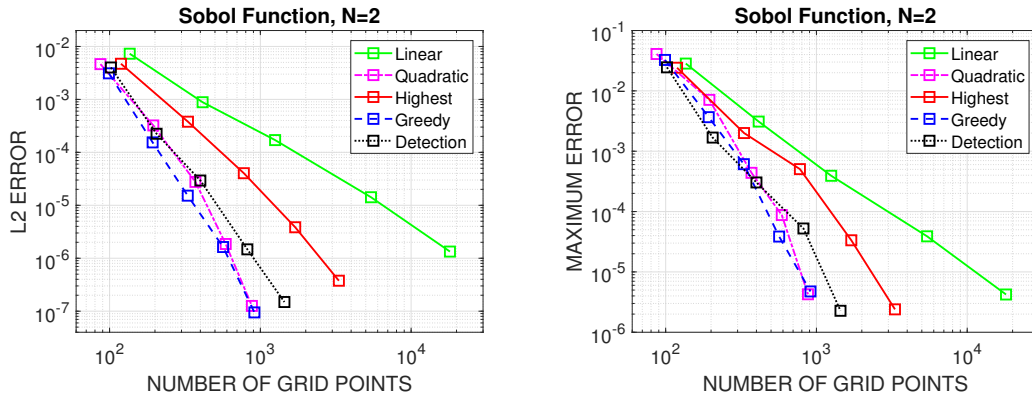


Figure 8: Test problem with f_2^2 . Comparison of the errors ϵ_2 (left) and ϵ_∞ (right).

4.4 Approximation of f_3^N in various dimensions

As a test of robustness and application to discontinuous functions, we finally consider f_3^N for $N = 2, 5$. The function has discontinuities along the lower-dimensional manifolds $x_1 = 0.51$ and $x_2 = 0.51$. Its approximation by continuous polynomials is characterized by the so-called Gibbs phenomenon which manifests itself in undesired over- and undershoots in the neighborhood of the discontinuities. Adaptivity and the use of linear polynomials close to the discontinuity can mitigate this effect. Although not designed for this case, we apply our kink detection approach with $w_{\text{kink}} = 1$ and without any further adaptation. The coefficients a_i are monotonically decreasing, which renders higher dimensions less important. The threshold w_{\max} for „quadratic“ varies in $[5 \cdot 10^{-9}, 5 \cdot 10^{-7}]$ and $[5 \cdot 10^{-9}, 10^{-5}]$

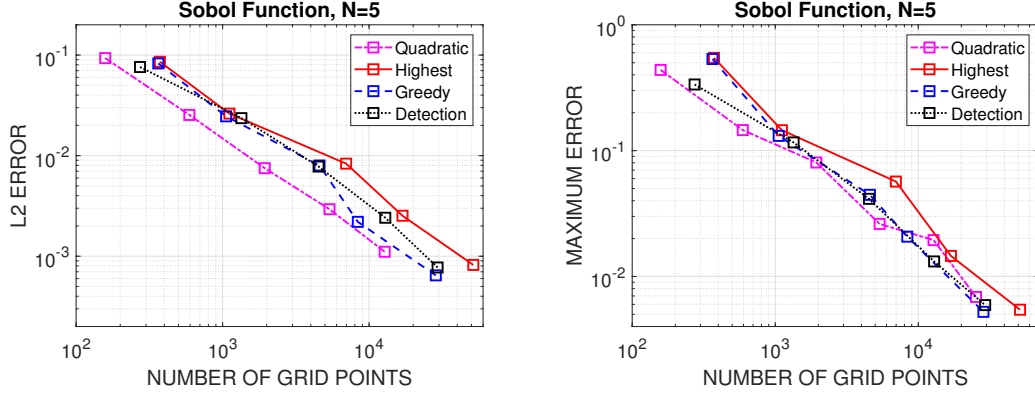


Figure 9: Test problem with f_2^5 . Comparison of the errors ϵ_2 (left) and ϵ_∞ (right).

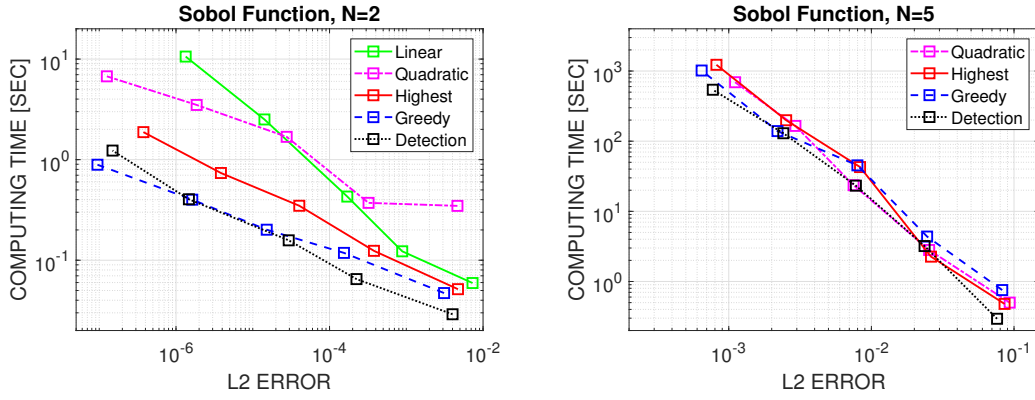


Figure 10: Test problem with f_2^N . Comparison of computing time in seconds versus accuracy in the 2-norm for $N = 2$ (left) and $N = 5$ (right).

for $N = 2$ and $N = 5$, respectively. For the other methods, we use the thresholds $w_{max} = 10^{-2}, 5 \cdot 10^{-3}, 10^{-3}, 5 \cdot 10^{-4}, 10^{-4}$, for $N = 2$ and these values multiplied by 10 for $N = 5$. In Figure 11 and Figure 12, we present results for the 2-norm only, since the ∞ -norm is not appropriate here. The simple method „linear“ performs quite well. It even shows quadratic order with respect to the reciprocal number of grid points in the case $N = 2$. For $N = 5$, it drops down to first order. However, in both test cases, the method is quite efficient with respect to computing time. Although not designed for discontinuous functions, *hp*-GSG-k delivers acceptable results and can keep up with „highest“. Both the greedy approach and „quadratic“ perform best and equally well with a small but visible advantage for the first one for $N = 5$. However, „quadratic“ is clearly outperformed in terms of computing times by all other methods. The reason is as follows: Its exploration of indices and identification of admissible points become more and more expensive for higher refinement levels which are required to accurately resolve the discontinuities.

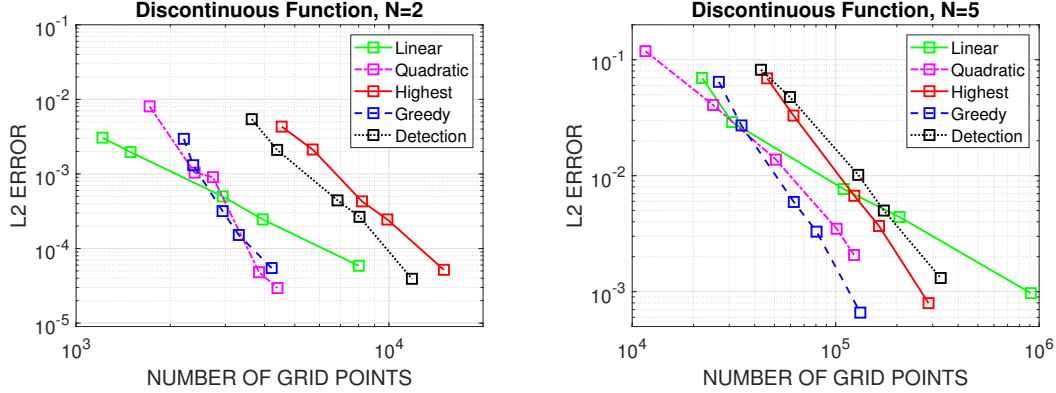


Figure 11: Test problem with f_3^N . Comparison of the errors ϵ_2 for $N = 2$ (left) and $N = 5$ (right).

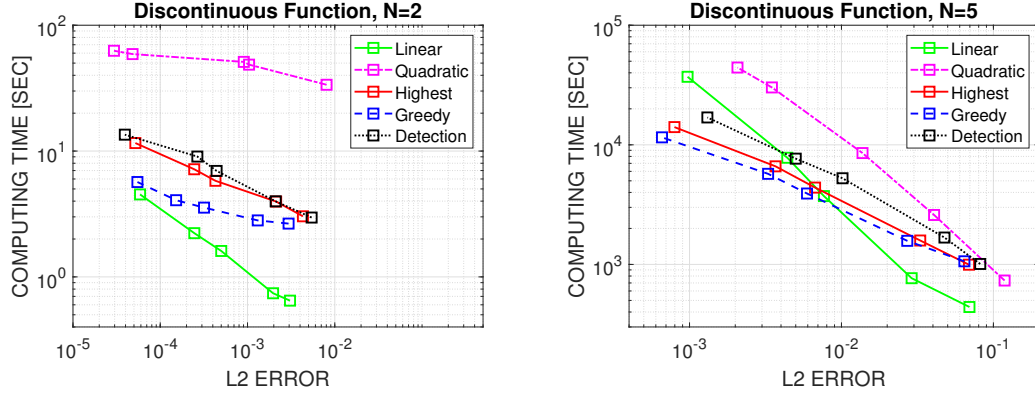


Figure 12: Test problem with f_3^N . Comparison of computing time versus accuracy in the 2-norm for $N = 2$ (left) and $N = 5$ (right).

5 Conclusion

In this paper, we have developed a novel *hp*-adaptive sparse grid collocation algorithm with spatial refinement for piecewise smooth functions with kinks along certain manifolds. Both the greedy and the kink detection approach perform equally well for three benchmark problems with continuous functions. In these cases, classical (isotropic) *h*-methods with multi-linear hierarchical basis functions or fixed maximum polynomial degree are clearly outperformed for higher dimensions with respect to the number of grid points necessary to achieve a certain accuracy as well as the corresponding computing time. The comparatively simple greedy strategy to select optimal local polynomial degrees works very efficient and robust. The kink detection algorithm has the potential for further improvements as can be seen for the high-dimensional Genz problem, but comes with the burden of an additional

appropriate choice of the threshold parameter w_{kink} . The anisotropic h -method with quadratic basis functions performs well in terms of accuracy per number of grid points, but often needs significantly higher computing time to detect important components and to check for admissible points. Its advantage in high dimensions with strong anisotropy is obvious as well as its deficiencies for the discontinuous function considered. Here, the hp -greedy method combines the merit of using linear polynomials in the neighborhood of the discontinuity and higher order polynomials elsewhere.

In future work, we will apply our stochastic collocation method to real gas network problems, where regulations of the gas flow yields kinks in certain quantities of interest as e.g. the maximum pressure over time at delivery exits. Efficient approximations of such quantities in higher dimensions will be one of the key steps to solve stochastic optimal control problems with probabilistic constraints.

Acknowledgements. Both authors are supported by the Deutsche Forschungsgemeinschaft (German Research Foundation) within the collaborative research center TRR154 “Mathematical modeling, simulation and optimisation using the example of gas networks” (Project-ID 239904186, TRR154/3-2022, TP B01).

Declaration of competing interest. The authors declare that they have no known competing financial interests or personal relationships that could have appeared to influence the work reported in this paper.

References

- [1] R. Archibald, A. Gelb, and J. Yoon. Polynomial fitting for edge detection in irregularly sampled signals and images. *SIAM J. Numer. Anal.*, 43:259–279, 2005.
- [2] R. Archibald, A. Gelb, and J. Yoon. Determining the locations of discontinuities in the derivatives of functions. *Appl. Numer. Math.*, 58:577–592, 2008.
- [3] H.-J. Bungartz. *Finite elements of higher order on sparse grids*. Habilitationsschrift. Institut für Informatik, TU München and Shaker Verlag, Aachen, 1998.
- [4] H.-J. Bungartz and M. Griebel. Sparse grids. *Acta Numer.*, 13:147–269, 2004.
- [5] B. Fuchs and J. Garcke. Simplex stochastic collocation for piecewise smooth functions with kinks. *International Journal for Uncertainty Quantification*, 10:1–24, 2020.
- [6] A. Genz. Testing multidimensional integration routines. In B. Ford, J.C. Rault, and F. Thomasset, editors, *International conference on tools, methods and languages for scientific and engineering computation*, pages 81–94. Elsevier North-Holland, Inc., 1984.

- [7] T. Gerstner and M. Griebel. Numerical integration using sparse grids. *Numer. Algorithms*, 18:209–232, 1998.
- [8] T. Gerstner and M. Griebel. Dimension-adaptive tensor-product quadrature. *Computing*, 71:65–87, 2003.
- [9] M. Griebel. Adaptive sparse grid multilevel methods for elliptic PDEs based on finite differences. *Computing*, 61:151–179, 1998.
- [10] J.D. Jakeman and S.G. Roberts. Local and dimension adaptive sparse grid interpolation and quadrature. Technical Report <https://arxiv.org/abs/1110.0010v1>, 2011.
- [11] A. Klimke. *Uncertainty Modeling using Fuzzy Arithmetic and Sparse Grids*. PhD thesis, Universität Stuttgart, Shaker Verlag, Aachen, 2006.
- [12] X. Ma and N. Zabararas. An adaptive hierarchical sparse grid collocation algorithm for the solution of stochastic differential equations. *J. Comput. Phys.*, 228:3084–3113, 2009.
- [13] F. Nobile, R. Tempone, and C. Webster. An anisotropic sparse grid stochastic collocation method for partial differential equations with random input data. *SIAM J. Numer. Anal.*, 46:2411–2442, 2008.
- [14] M. Obersteiner and H.-J. Bungartz. A generalized spatially adaptive sparse grid combination technique with dimension-wise refinement. *SIAM J. Sci. Comput.*, 43:A2381–A2403, 2021.
- [15] A. Saltelli and I.M. Sobol. Sensitivity analysis for nonlinear mathematical models: numerical experience. *Matem. Mod.*, 7:16–28, 1995.
- [16] S. Smolyak. Quadrature and interpolation formulas for tensor product of certain classes of functions. *Soviet Math. Dokl.*, 4:240–243, 1963.
- [17] Z. Tao, Y. Jiang, and Y. Cheng. An adaptive high-order piecewise polynomial based sparse grid collocation method with applications. *J. Comput. Phys.*, 433:109770, 2021.
- [18] C. Zenger. Sparse grids. In W. Hackbusch, editor, *Parallel Algorithms for Partial Differential Equations*, volume 31 of *Notes Numer. Fluid Mech*, pages 241–251. Vieweg, Brunswick, Germany, 1991.